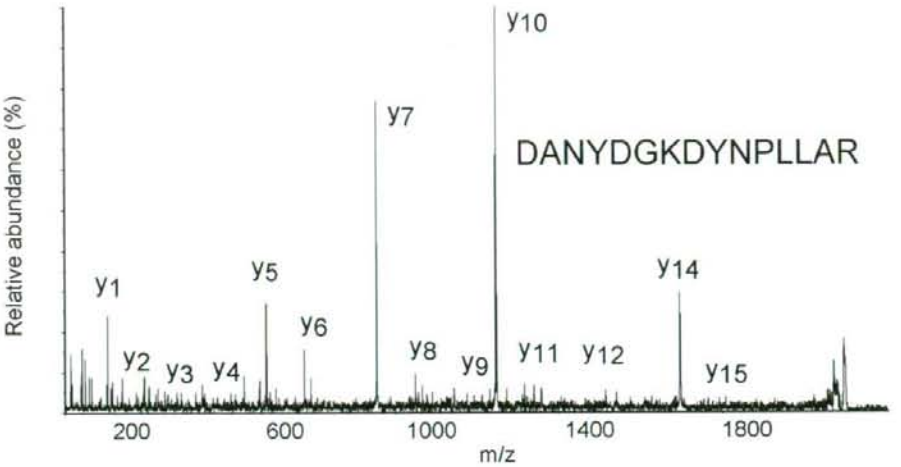

Figure 3 Identification of EB3 by MS/MS. An MS/MS spectrum of one peptide corresponded to the sequence DANYDGKDYNPLLAR of EB3. Predicted C-terminal fragments are marked as y.

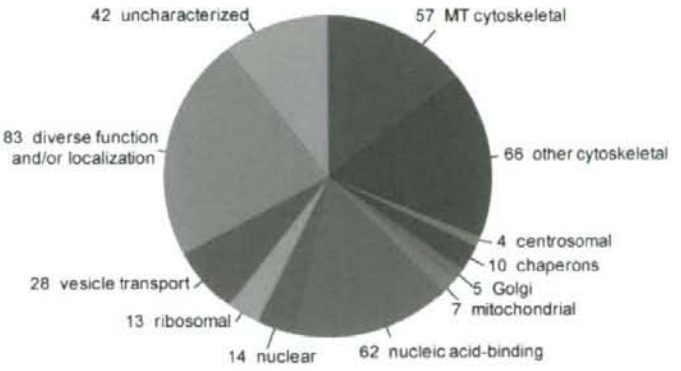

Figure 4 Classification of identified proteins. Absolute numbers are indicated.

Identification of novel components of centrosomes and cilia

We identified many proteins that had not been previously characterized. These proteins are intriguing candidates for being involved in MT-based functions and structures. Homology analysis indicated that these uncharacterized proteins, except MAP7 domain-containing proteins 1 and 2, did not show obvious homology to known proteins and did not contain functional motifs or domains. MAP7 domain-containing proteins 1 and 2 possessed a domain with a sequence similar to the MT-binding site of MAP7 (data not shown). It is plausible that these proteins function as MAPs. Apart from these MAP candidates, six novel gene products were chosen for further characterization because their cDNAs were available (Table 2). These gene products were expressed as N-terminal enhanced green fluorescent protein (EGFP)-fused proteins in the retina pigment epithelium RPE-1 cells. The localization of expressed proteins was examined by indirect immunofluorescence microscopy. Of the six proteins analyzed, FLJ21438 and the hypothetical protein (Q96MC5) showed a vesicular staining pattern whereas LRRC40 showed a cytoplasmic staining pattern (data not shown). On the other hand, KIAA1505 and LRRC45, both of which contained coiled-coil domains, were

© 2008 The Authors
Journal compilation © 2008 by the Molecular Biology Society of Japan/Blackwell Publishing Ltd.

Table 1 List of identified proteins

	Name	Accession No.	Categories	Fraction
1	Bicaudal D homologue 2	Q921C5	MT-binding	S
2	Bullous pemphigoid antigen 1 isoform	Q03001	MT-binding	S, E
3	CH-TOG protein	Q14008	MT-binding	S, E
4	CLIP-115	Q9Z0H8	MT-binding	S, E
5	CLIP-170	Q9JK25	MT-binding	E
6	Echinoderm microtubule-associated protein like 2	Q7TNG5	MT-binding	E
7	E-STOP protein	O88748	MT-binding	S
8	Growth-arrest-specific protein 8	O95995	MT-binding	E
9	Hook homologue 1	Q8BIL5	MT-binding	S
10	Hook homologue 3	Q86VS8	MT-binding	S
11	KARP-1-binding protein 2	Q5SW79	MT-binding	S
12	Microtubule-actin cross-linking factor 1, isoform 4	Q9UPN3	MT-binding	S
13	Microtubule-associated protein 1A	P78559	MT-binding	S, E
14	Microtubule-associated protein 1B	P15205	MT-binding	E
15	Microtubule-associated protein 2	P15146	MT-binding	S, E
16	Microtubule-associated protein 6	Q6P3T0	MT-binding	S
17	Microtubule-associated protein EMAP	Q6P6T4	MT-binding	E
18	Microtubule-associated protein RP/EB family member 1	Q15691	MT-binding	S, E
19	Microtubule-associated protein RP/EB family member 3	Q9UPY8	MT-binding	S, E
20	Microtubule-associated protein τ	P19332	MT-binding	S, E
21	Microtubule-associated serine/threonine-protein kinase 1	Q810W7	MT-binding	S
22	Plectin	Q15149	MT-binding	S, E
23	Restin	Q922J3	MT-binding	S
24	Serine/threonine-protein kinase DCAMKL1	O15075	MT-binding	S, E
25	Serine/threonine-protein kinase DCAMKL2	Q8N568	MT-binding	E
26	Serine/threonine-protein kinase MARK1	O08678	MT-binding	S
27	Treacle protein	Q13428	MT-binding	S
28	Tubulin α1	P68361	MT-binding	S, E
29	Tubulin α2	P05213	MT-binding	E
30	Tubulin α3	Q71U36	MT-binding	S, E
31	Tubulin α6	Q9BQE3	MT-binding	S, E
32	Tubulin α8	Q9JJZ2	MT-binding	E
33	Tubulin β1	Q9H4B7	MT-binding	E
34	Tubulin β2	P07437	MT-binding	S, E
35	Tubulin β3	Q9ERD7	MT-binding	S, E
36	Tubulin β4	Q9D6F9	MT-binding	S, E
37	Tubulin β5	P99024	MT-binding	E
38	Tubulin polymerization-promoting protein	Q27957	MT-binding	E
39	Tumor-associated microtubule-associated protein	Q8WWK9	MT-binding	S
40	Dynactin 1	O08788	MT-motor	S, E
41	Dynactin 2	Q99KJ8	MT-motor	E
42	Dynactin 4	Q9QUR2	MT-motor	S
43	Dynein heavy chain	P38650	MT-motor	S
44	Dynein intermediate chain 1	Q63100	MT-motor	S
45	Dynein light intermediate chain 2	Q62698	MT-motor	S
46	KIF1B	Q60575	MT-motor	S
47	KIF2	P28740	MT-motor	S, E
48	KIF3A	P28741	MT-motor	E
49	KIF3B	Q61771	MT-motor	E
50	KIF3C	O55165	MT-motor	E
51	KIF5A	Q12840	MT-motor	S
52	KIF5B	Q61768	MT-motor	E
53	KIF5C	O60282	MT-motor	E
54	Kinesin light chain 1	Q07866	MT-motor	S, E

Continued overleaf

© 2008 The Authors
Journal compilation © 2008 by the Molecular Biology Society of Japan/Blackwell Publishing Ltd.

Table 1 *Continued*

	Name	Accession No.	Categories	Fraction
55	Kinesin light chain 2	O88448	MT-motor	S, E
56	Kinesin-associated protein 3	P70188	MT-motor	S
57	Actin α2	Q13707	Other-cytoskeleton	S, E
58	Actin β	P60709	Other-cytoskeleton	S, E
59	Actin γ	P63261	Other-cytoskeleton	S, E
60	α-Actinin 1	P12814	Other-cytoskeleton	E
61	α-Actinin 4	Q96BG6	Other-cytoskeleton	E
62	Ankyrin 2	Q01484	Other-cytoskeleton	S
63	Ankyrin 3	Q8VC68	Other-cytoskeleton	E
64	Ankyrin G	O70511	Other-cytoskeleton	E
65	Band 4.1-like protein 2	O70318	Other-cytoskeleton	E
66	Capping protein α1	P47753	Other-cytoskeleton	E
67	Capping protein α2	Q3T1K5	Other-cytoskeleton	E
68	Capping protein α3	Q9WUV6	Other-cytoskeleton	E
69	Cenexin 1	Q9JIZ4	Other-cytoskeleton	S
70	Cenexin 2	Q6AYX5	Other-cytoskeleton	E
71	Centractin	Q8R3C5	Other-cytoskeleton	S
72	Drebrin A	Q07266	Other-cytoskeleton	S
73	Ezrin	Q9UJZ6	Other-cytoskeleton	S
74	Filamin-interacting protein L—FILIP	Q8K4T4	Other-cytoskeleton	E
75	Glial fibrillary acidic protein α	P47819	Other-cytoskeleton	E
76	Keratin, type I cytoskeletal 17	Q04695	Other-cytoskeleton	S
77	Keratin, type I cytoskeletal 9	P35527	Other-cytoskeleton	E
78	Keratin, type I, cytoskeletal 10 epidermal	P13654	Other-cytoskeleton	E
79	Keratin, type II cytoskeletal 1	P04264	Other-cytoskeleton	E
80	Keratin, type II cytoskeletal 2 epidermal	P35908	Other-cytoskeleton	E
81	Keratin, type II cytoskeletal 4	P19013	Other-cytoskeleton	E
82	Keratin, type II cytoskeletal 6B	P04259	Other-cytoskeleton	E
83	Keratin, type II cytoskeletal 8	P11679	Other-cytoskeleton	E
84	Meiosis-specific nuclear structural protein 1	Q61884	Other-cytoskeleton	E
85	Moesin	P26042	Other-cytoskeleton	S
86	Nebulette	O76041	Other-cytoskeleton	E
87	Nebulin, skeletal muscle	P20929	Other-cytoskeleton	E
88	Neurofibromatosis type 2	P35240	Other-cytoskeleton	E
89	Neurofilament triplet H protein	P19246	Other-cytoskeleton	S
90	Neurofilament triplet L protein	P08551	Other-cytoskeleton	S
91	Neurofilament triplet M protein	P12839	Other-cytoskeleton	S
92	Nexilin	Q0ZGT2	Other-cytoskeleton	S, E
93	Peripherin	P21807	Other-cytoskeleton	S
94	Periplakin	Q9R269	Other-cytoskeleton	E
95	Radixin	P26044	Other-cytoskeleton	S
96	Septin-11	Q8C1B7	Other-cytoskeleton	E
97	Septin-2	Q15019	Other-cytoskeleton	S, E
98	Septin-3	Q9UH03	Other-cytoskeleton	S
99	Septin-6	Q9R1T4	Other-cytoskeleton	S
100	Septin-7	Q9WVC0	Other-cytoskeleton	S
101	Septin-9	Q9QZR6	Other-cytoskeleton	S
102	Spectrin α-chain	Q13813	Other-cytoskeleton	S, E
103	Spectrin β-chain	Q62261	Other-cytoskeleton	S, E
104	TPR protein	Q9UE33	Other-cytoskeleton	S, E
105	Trichoplein keratin filament-binding protein	Q9BT92	Other-cytoskeleton	E
106	Tropomodulin 2	Q9JKK7	Other-cytoskeleton	S, E
107	Tropomyosin 4	Q5U0D9	Other-cytoskeleton	S
108	Tropomyosin α	Q923Z2	Other-cytoskeleton	E
109	Tropomyosin β	P58775	Other-cytoskeleton	S, E

Continued overleaf

© 2008 The Authors
Journal compilation © 2008 by the Molecular Biology Society of Japan/Blackwell Publishing Ltd.

Table 1 *Continued*

	Name	Accession No.	Categories	Fraction
110	Tropomyosin γ	Q8K0Z5	Other-cytoskeleton	E
111	Type II brain 4.1	Q9JMB3	Other-cytoskeleton	S
112	Vimentin	P08670	Other-cytoskeleton	S, E
113	Wasp family 1	Q8R5H6	Other-cytoskeleton	S
114	M-phase phosphoprotein 1	Q96Q89	Motor	E
115	Myosin Va	Q9Y4I1	Motor	E
116	Myosin Vb	Q9ULV0	Motor	S
117	Myosin, heavy polypeptide 10	P35580	Motor	S
118	Myosin, heavy polypeptide 11	O08638	Motor	S, E
119	Myosin, heavy polypeptide 13	Q9GJP9	Motor	E
120	Myosin, heavy polypeptide 14	Q7Z406	Motor	S
121	Myosin, heavy polypeptide 16	Q9H6N6	Motor	E
122	Myosin, heavy polypeptide 7	Q91Z83	Motor	E
123	Myosin, heavy polypeptide 9	P35579	Motor	S, E
124	AKAP 450	Q99996	Centrosome	S
125	Centrosomal protein Cep290	O15078	Centrosome	S, E
126	Oral–facial–digital syndrome 1 protein	O75665	Centrosome	E
127	Rootletin	CROCC	Centrosome	E
128	78 kDa glucose-regulated protein	P34935	Chaperone	S, E
129	DnaJ (Hsp40) homologue, subfamily A, member 2	Q9QYJ0	Chaperone	E
130	DnaJ (Hsp40) homologue, subfamily B, member 14	Q8TBM8	Chaperone	E
131	Heat shock cognate 71 kDa protein	P11142	Chaperone	S, E
132	Heat shock protein HSP 90-α	P07901	Chaperone	S
133	Heat shock-related 70 kDa protein 2	P54652	Chaperone	E
134	Heat shock-related 70 kDa protein 4	O88600	Chaperone	S
135	Orp150 (150 kDa oxygen-regulated protein precursor)	Q63617	Chaperone	S
136	Stress-induced-phosphoprotein 1	O35814	Chaperone	S
137	THEG protein	Q9P2T0	Chaperone	S
138	Giantin	Q14789	Golgi	E
139	Golgin-245	Q13439	Golgi	S, E
140	Optineurin	Q96CV9	Golgi	S
141	PACS-1	O88588	Golgi	S
142	Rat GCP360	Q63714	Golgi	E
143	ADP–ATP translocase 3	P32007	Mitochondria	E
144	ADP–ATP translocase 4	Q9H0C2	Mitochondria	E
145	ATPase inhibitor precursor, mitochondrial	Q9UII2	Mitochondria	S
146	Mitochondrial ribosomal protein L51	Q9CPY1	Mitochondria	S
147	Peroxiredoxin V (PrxV) protein	Q9JHL8	Mitochondria	S
148	Solute carrier family 25, member 5	Q545A2	Mitochondria	S
149	Vacuolar adenosine triphosphatase subunit A	P50516	Mitochondria	S
150	APEX nuclease	P27695	NA-binding	S
151	Cell growth regulating nucleolar protein LYAR	Q08288	NA-binding	S
152	DEAD box polypeptide 27	Q96GQ7	NA-binding	E
153	DEAD box protein RB	Q92499	NA-binding	S
154	DNA cytosine methyltransferase 3α	Q9Y6K1	NA-binding	E
155	DNA polymerase κ	Q9UBT6	NA-binding	S
156	DNA repair protein RAD50	P70388	NA-binding	E
157	DNA topoisomerase I	Q07050	NA-binding	E
158	DNA topoisomerase IIα	O55078	NA-binding	E
159	DNA-dependent ATPase SNF2L	Q6PGB8	NA-binding	E
160	ETOILE	Q9R226	NA-binding	E
161	Heat shock transcription factor 2	Q9BS48	NA-binding	E
162	Heterogeneous nuclear ribonucleoprotein A1	P09651	NA-binding	S
163	Heterogeneous nuclear ribonucleoprotein A2/B	O88569	NA-binding	S
164	Heterogeneous nuclear ribonucleoprotein A3	Q8BG05	NA-binding	S

Continued overleaf

© 2008 The Authors
Journal compilation © 2008 by the Molecular Biology Society of Japan/Blackwell Publishing Ltd.

Table 1 *Continued*

	Name	Accession No.	Categories	Fraction
165	Heterogeneous nuclear ribonucleoprotein G	O97560	NA-binding	S
166	Heterogeneous nuclear ribonucleoprotein K	P61978	NA-binding	E
167	Heterogeneous nuclear ribonucleoprotein M	Q9D0E1	NA-binding	S, E
168	Heterogeneous nuclear ribonucleoprotein R	Q99KG1	NA-binding	E
169	Heterogeneous nuclear ribonucleoprotein U	Q63555	NA-binding	S, E
170	Homeobox protein TGIF2LX	Q8MID8	NA-binding	S
171	KH domain containing, RNA binding, signal transduction-associated 1	Q07666	NA-binding	E
172	KRAB-A interacting protein	Q62318	NA-binding	S
173	LLDBP	Q14756	NA-binding	S
174	Microphthalmia-associated transcription factor	O88368	NA-binding	S
175	Minor histocompatibility antigen HA-8	Q15397	NA-binding	E
176	Myelin transcription factor 1-like protein	Q9UL68	NA-binding	S
177	Non-POU-domain-containing, octamer binding protein	Q99K48	NA-binding	S
178	Nucleolar transcription factor 1	P25977	NA-binding	S
179	Origin recognition complex subunit 1	Q9JI69	NA-binding	S
180	Plasminogen activator inhibitor 1 RNA-binding protein	Q8NC51	NA-binding	S, E
181	RENT1	Q9EPU0	NA-binding	S
182	Ribonuclease 4	P34096	NA-binding	S
183	RNA-binding protein 27	Q5SFM8	NA-binding	S
184	RNA-binding protein 5	P52756	NA-binding	E
185	RNA-binding protein 6	P78332	NA-binding	S
186	SOX-10	P56693	NA-binding	E
187	SOX-21	Q811W0	NA-binding	E
188	Splicing co-activator subunit SRm300	Q9UQ35	NA-binding	S
189	Splicing factor 3 subunit 1	Q8K4Z5	NA-binding	E
190	Splicing factor, arginine/serine-rich 6	Q6GL71	NA-binding	S
191	Splicing factor, proline- and glutamine-rich, SFPQ	Q8VIJ6	NA-binding	S, E
192	Structural maintenance of chromosome 1-like 1 protein	Q9CU62	NA-binding	S, E
193	Structural maintenance of chromosome 2-like 1 protein	O95347	NA-binding	S
194	Structural maintenance of chromosomes 5-like 1	Q8CG46	NA-binding	E
195	Structural maintenance of chromosomes 6-like 1	Q96SB8	NA-binding	E
196	Surfeit locus protein 6	P70279	NA-binding	S
197	SWI/SNF complex 170 kDa subunit	Q8TAQ2	NA-binding	S
198	Sucrose non-fermenting protein 2 homologue	Q91ZW3	NA-binding	S
199	Synaptonemal complex protein 1	Q03410	NA-binding	S, E
200	Synaptonemal complex protein 2	Q9BX26	NA-binding	E
201	T-box transcription factor TBX3	O15119	NA-binding	S
202	Transcription elongation factor A protein 1	P23193	NA-binding	S
203	Transcription elongation regulator 1	O14776	NA-binding	E
204	Transcription factor LUZP	Q9ESV1	NA-binding	E
205	Tumor protein p73-like	Q9JJP6	NA-binding	S
206	Vascular actin single-stranded DNA-binding factor 2 p44 component	O35295	NA-binding	S
207	Vitamin D response element binding protein	Q9TTV2	NA-binding	S
208	Zinc finger protein 40	Q06054	NA-binding	E
209	Zinc finger protein 62 homologue	Q8NB50	NA-binding	E
210	Zinc finger protein 85	Q03923	NA-binding	S
211	Zinc finger protein 92	Q03936	NA-binding	S
212	Abnormal spindle-like microcephaly-associated protein	Q8IZT6	Nuclear	S, E
213	Brain-expressed X-linked protein 1	Q9R224	Nuclear	E
214	Cell proliferation antigen Ki-67, short form	P46013	Nuclear	E
215	Centrosomin B	P23116	Nuclear	E
216	Chmadrin	Q9XS53	Nuclear	S
217	Desmoyokin	Q09666	Nuclear	S
218	KARP-1-binding protein 1	Q91Y79	Nuclear	S
219	KRAB-zinc finger protein KID3	Q571J5	Nuclear	S

Continued overleaf

© 2008 The Authors
Journal compilation © 2008 by the Molecular Biology Society of Japan/Blackwell Publishing Ltd.

Table 1 *Continued*

	Name	Accession No.	Categories	Fraction
220	Lamin A/C	P02545	Nuclear	E
221	Matrin 3	P43243	Nuclear	E
222	Nesprin 1	Q8NF91	Nuclear	S
223	Rbm	Q60990	Nuclear	E
224	Uveal autoantigen	Q9BG87	Nuclear	S, E
225	Zinc finger protein DZIP1	Q8BMD2	Nuclear	E
226	Eukaryotic initiation factor 4A-I	P29562	Ribosomal	E
227	Eukaryotic initiation factor 4A-II	Q14240	Ribosomal	E
228	Eukaryotic translation initiation factor 2 subunit 1	P68101	Ribosomal	S
229	Eukaryotic translation initiation factor 2 subunit 2	Q99L45	Ribosomal	E
230	Eukaryotic translation initiation factor 3 subunit 10	Q14152	Ribosomal	E
231	Eukaryotic translation initiation factor 4-γ2	Q62448	Ribosomal	S
232	Ribosomal protein L3	P39023	Ribosomal	S
233	Ribosomal protein L35a	Q9DC85	Ribosomal	E
234	Ribosomal protein L4	Q9D8E6	Ribosomal	S
235	Ribosomal protein L7	P18124	Ribosomal	E
236	Ribosomal protein S11	P62280	Ribosomal	E
237	Ribosome-binding protein 1	Q9P2E9	Ribosome	S, E
238	Small nuclear ribonucleoprotein component U5	Q15029	Ribosomal	S
239	Adaptor-related protein complex AP-4 σ4 subunit	Q9Y587	Vesicle	S
240	Charged multivesicular body protein 2b	Q9UQN3	Vesicle	S
241	Clathrin heavy chain	P49951	Vesicle	S, E
242	Clathrin light chain B	P08082	Vesicle	E
243	Dynamin 1	P39053	Vesicle	S, E
244	Early endosome antigen 1	Q15075	Vesicle	S, E
245	ERC protein 2	Q8K3M6	Vesicle	E
246	Exocyst complex component 7	Q9UPT5	Vesicle	S
247	Flotillin-1	O75955	Vesicle	S
248	Kinectin	Q86UP2	Vesicle	E
249	Plasmalemma vesicle-associated protein	Q91VC4	Vesicle	S
250	PV1 (Plasmalemma vesicle-associated protein)	Q9BX97	Vesicle	S, E
251	Rab GDP dissociation inhibitor2	O97556	Vesicle	S
252	RAB11 family interacting protein 4	Q86YS3	Vesicle	E
253	Rab2, GTP-binding protein Rab2	P61019	Vesicle	S
254	Rab6-interacting protein 2	Q99MI1	Vesicle	S, E
255	Rabphilin-3A	P47708	Vesicle	E
256	RUN and FYVE domain-containing protein 2	Q8R4C2	Vesicle	S, E
257	SH3 domain protein 2A	Q62420	Vesicle	S
258	Soluble NSF attachment protein α	P54921	Vesicle	E
259	Soluble NSF attachment protein β	Q8N8N1	Vesicle	S, E
260	Soluble NSF attachment protein γ	Q99747	Vesicle	E
261	Synapsin IIa	Q63537	Vesicle	E
262	Synapsin IIb	Q92777	Vesicle	E
263	Synapsin-1	P09951	Vesicle	S
264	Synaptojanin 2	Q9D2G5	Vesicle	S
265	Synaptotagmin-like protein 3	Q99N48	Vesicle	S
266	Transitional endoplasmic reticulum ATPase	P46462	Vesicle	S
267	14-3-3 protein β/α	P31946	Diverse	E
268	14-3-3 protein η	P68510	Diverse	E
269	14-3-3 protein γ	P68252	Diverse	E
270	14-3-3 protein ζ/δ	P63102	Diverse	E
271	14-3-3 protein, ε	P62260	Diverse	E
272	14-3-3 protein, θ	P68255	Diverse	E
273	26S protease regulatory subunit 8	P62198	Diverse	E
274	26S proteasome non-ATPase regulatory subunit 12	Q9D8W5	Diverse	E
275	Activation-induced cytidine deaminase	Q8NFC4	Diverse	E
276	α-Internexin	P46660	Diverse	E
277	ARF GTPase-activating protein GIT1	Q9Z272	Diverse	S

Continued overleaf

© 2008 The Authors
Journal compilation © 2008 by the Molecular Biology Society of Japan/Blackwell Publishing Ltd.

Table 1 *Continued*

	Name	Accession No.	Categories	Fraction
278	Ca^{2+}/calmodulin-dependent protein kinase II β-chain	P08413	Diverse	S
279	cAMP-dependent protein kinase type II-α regulatory chain	Q8K1M3	Diverse	S
280	cAMP-dependent protein kinase type II-β regulatory subunit	P12369	Diverse	S
281	cAMP-dependent protein kinase, α-catalytic subunit	Q9MZD9	Diverse	S
282	cAMP-dependent protein kinase, β-catalytic subunit	P22694	Diverse	E
283	Carboxy terminus of HSP70-interacting protein	Q9UNE7	Diverse	S
284	Carnitine deficiency-associated protein expressed in ventricle 1	Q8WYA0	Diverse	E
285	Caskin-1	Q8VHK2	Diverse	E
286	Caspase-1	Q9TV13	Diverse	E
287	CENP-F kinetochore protein	P49454	Diverse	E
288	Citron ρ-interacting kinase	P49025	Diverse	S, E
289	Coiled-coil and C2 domain-containing protein 1A	Q8K1A6	Diverse	S
290	CUB and sushi multiple domains protein 2	Q7Z408	Diverse	S, E
291	Cullin-4B	Q13620	Diverse	S
292	Cytochrome *c* oxidase assembly protein COX19	Q8K0C8	Diverse	E
293	Cytochrome P450 2D6	P10635	Diverse	S
294	Dendrotoxin α-dendrotoxin-sensitive potassium channel β	Q27955	Diverse	E
295	Desmoplakin	P15924	Diverse	E
296	Diacylglycerol kinase γ	P49619	Diverse	S
297	Dihydrolipoyllysine-residue acetyltransferase component of pyruvate dehydrogenase complex	P08461	Diverse	S, E
298	Dual-specificity tyrosine-phosphorylation regulated kinase 2	Q92630	Diverse	S
299	DVL-binding protein DAPLE	Q6VGS5	Diverse	E
300	Filamin A interacting protein 1	Q7Z7B0	Diverse	E
301	Focal adhesion kinase 1	P34152	Diverse	S
302	Fructose-bisphosphate aldolase A	P05065	Diverse	S, E
303	Fructose-bisphosphate aldolase C	P09972	Diverse	S
304	G protein-coupled receptor-associated sorting protein 1	Q5U4C1	Diverse	E
305	Glutamine synthetase	P09606	Diverse	S
306	Glyceraldehyde-3-phosphate dehydrogenase	P04797	Diverse	S
307	Glycogen synthase kinase-3α	P49840	Diverse	S
308	Glycogen synthase kinase-3β	P18266	Diverse	S
309	Glycosyl-phosphatidyl-inositol-anchored protein p137-like	Q6YF16	Diverse	E
310	GRIN1	Q3UNH4	Diverse	E
311	Hexokinase 1	Q91W97	Diverse	E
312	Liprin α1	Q13136	Diverse	S
313	Liprin α4	Q91Z80	Diverse	S
314	Membrane-associated progesterone receptor component 1	O00264	Diverse	S
315	Mirror-image polydactyly gene 1 protein	Q8TD10	Diverse	S, E
316	Myotubularin-related protein 8	Q96EF0	Diverse	S
317	N2B-titin isoform	Q8WZ42	Diverse	S
318	Nasopharyngeal epithelium specific protein 1	Q9D9U9	Diverse	S
319	Nebulin-related anchoring protein	Q86VF7	Diverse	S
320	Osmosis responsive factor	Q6PID6	Diverse	S, E
321	Proliferation potential-related protein	Q7Z6E9	Diverse	S
322	Proteasome subunit α-type 1	P25786	Diverse	S, E
323	Proteasome subunit α-type 4	Q9R1P0	Diverse	S
324	Protein kinase C inhibitor KCIP-1 isoform δ	Q7M332	Diverse	S
325	Protein kinase C-α binding protein	Q9NRD5	Diverse	S
326	Protein phosphatase 2, α-isoform of regulatory subunit A	P30153	Diverse	S
327	Pyruvate dehydrogenase E1 component α-subunit	P08559	Diverse	S
328	Ras-GTPase-activating protein binding protein 2	P97379	Diverse	S, E
329	Receptor tyrosine kinase-like orphan receptor 2	Q9Z138	Diverse	S
330	Regulator of G protein signaling protein	Q86UV0	Diverse	S
331	ρ/rac guanine nucleotide exchange factor (GEF) 2	Q60875	Diverse	S
332	ρ-associated protein kinase 1	Q63644	Diverse	S, E
333	ρ-associated protein kinase 2	Q62868	Diverse	S, E

Continued overleaf

© 2008 The Authors
Journal compilation © 2008 by the Molecular Biology Society of Japan/Blackwell Publishing Ltd.

Table 1 *Continued*

	Name	Accession No.	Categories	Fraction
334	Ribosomal protein S6 kinase α5	O75582	Diverse	S
335	RING finger protein 20	Q5VTR2	Diverse	S
336	SAD1 kinase	Q8TDC3	Diverse	S
337	Serine/threonine kinase 10	Q62830	Diverse	E
338	SSX5 protein	O60225	Diverse	S
339	Staphylococcal nuclease domain containing 1	Q7KZF4	Diverse	E
340	STIP1 homology and U-Box containing protein 1	Q9WUD1	Diverse	S
341	Transcription elongation factor B polypeptide 3 binding protein 1	Q8N1G1	Diverse	S
342	Tripartile motif protein2	Q9ESN6	Diverse	S
343	Tripartile motif protein46	Q95J41	Diverse	S
344	tRNA pseudouridine synthase A	Q9WU56	Diverse	E
345	Testis-specific gene 10 protein	Q9BZW7	Diverse	S
346	Uaca protein	Q8CIA8	Diverse	S
347	Voltage-gated potassium channel β-2 subunit	P62482	Diverse	S
348	X-ray repair complementing defective repair in Chinese hamster cells 5	Q8C4N6	Diverse	S
349	Zinc finger FYVE domain containing protein 19	Q96K21	Diverse	S
350	BC004690 protein	Q99KF2	Uncharacterized	S
351	C6orf97 protein	Q8IYT3	Uncharacterized	E
352	CGI-62 protein	Q96GY0	Uncharacterized	S
353	Coiled-coil domain containing protein 13	Q8IYE1	Uncharacterized	S, E
354	Coiled-coil domain containing protein 9	Q8VC31	Uncharacterized	S
355	FLJ21438 protein	Q8N2T9	Uncharacterized	E
356	Hypothetical	Q68DY1	Uncharacterized	E
357	Hypothetical	Q9UFB7	Uncharacterized	E
358	Hypothetical	Q95JK1	Uncharacterized	E
359	Hypothetical	Q96DK7	Uncharacterized	E
360	Hypothetical	Q96LI9	Uncharacterized	E
361	Hypothetical	Q9H943	Uncharacterized	E
362	Hypothetical	Q8K303	Uncharacterized	E
363	Hypothetical	Q5T655	Uncharacterized	E
364	Hypothetical	Q95JL6	Uncharacterized	E
365	Hypothetical	Q9BE47	Uncharacterized	E
366	Hypothetical	Q9NXG0	Uncharacterized	E
367	Hypothetical	Q8N8E3	Uncharacterized	E
368	Hypothetical	Q9NWK9	Uncharacterized	E
369	Hypothetical	Q96LP2	Uncharacterized	E
370	LRRC40 (Leucine-rich repeat-containing protein 40)	Q9CRC8	Uncharacterized	S
371	Hypothetical	Q6NZL0	Uncharacterized	S
372	Hypothetical	Q95JX8	Uncharacterized	S
373	Hypothetical	Q96MC5	Uncharacterized	E
374	Hypothetical	Q9D4V3	Uncharacterized	E
375	Hypothetical protein DKFZp434C196	Q9UF83	Uncharacterized	S
376	Hypothetical protein DKFZp564J047	Q5T0J7	Uncharacterized	S
377	Hypothetical, GRINL1A combined protein isoform 7	Q96NF5	Uncharacterized	S
378	Hypothetical, RIKEN cDNA 1700001L19	Q9DAR0	Uncharacterized	E
379	KIAA0542 protein	O60289	Uncharacterized	S
380	KIAA0692 protein	Q86XL3	Uncharacterized	S
381	KIAA1505 protein	Q8IYE0	Uncharacterized	E
382	CCDC40/KIAA1640 protein	Q8BI79	Uncharacterized	S, E
383	KIAA1937 protein	Q96PV1	Uncharacterized	E
384	LRRC45 (Leucine-rich repeat-containing protein 45)	Q8CIM1	Uncharacterized	E
385	MAP7 domain-containing protein 1	A2AJI0	Uncharacterized	S
386	MAP7 domain-containing protein 2	Q96T17	Uncharacterized	S, E
387	Protein C10orf118	Q7Z3E2	Uncharacterized	E
388	Protein C14orf145	Q6ZU80	Uncharacterized	E
389	RIKEN cDNA 2010300C02	Q9D852	Uncharacterized	E
390	Spermatogenesis-associated serine-rich protein 2	Q86XZ4	Uncharacterized	S
391	Uncharacterized protein C2orf16	Q68DN1	Uncharacterized	S

E, extract fraction; NA, uncleic acid; S, soluble fraction.

© 2008 The Authors
Journal compilation © 2008 by the Molecular Biology Society of Japan/Blackwell Publishing Ltd.

Table 2 Characterization of six unknown proteins

Name	Accession No.	Size (amino acids)	Domain	Localization
FLJ21438	Q8N2T9	264	None	Vesicular
LRRC40	Q9CRC8	602	LRR	Cytoplasmic
Hypothetical	Q96MC5	204	None	Vesicular
KIAA1505	Q8IYE0	955	CC	Centrosomes
CCDC40/KAA1640	Q8BI79	1192	CC	Cilia
LRRC45	Q8CIM1	670	CC/LRR	Centrosomes

LRR, leucine-rich repeat domain; CC, coiled-coil domain.

Figure 5 Structures of three uncharacterized proteins. CC, coiled-coil domain; and LRR, leucine-rich repeat domain.

co-localized with the centrosomal protein γ-tubulin (Figs 5 and 6). These results indicate that these two proteins are novel components of centrosomes.

CCDC40/KIAA1640 also contained coiled-coil domains (Fig. 5). This protein was co-localized with acetylated tubulin in RPE-1 cells (Fig. 6). Acetylated tubulin is known as a marker protein for detection of the primary cilia (Pipemo & Fuller 1985). To confirm the localization of CCDC40, this protein was expressed in MDCK cells grown on 7-day post-confluence. The staining pattern of CCDC40 was similar to that of acetylated tubulin (Fig. 7). Taken together, these results indicate that CCDC40 is a novel component of cilia.

Discussion

We analyzed MT co-sedimented proteins by MS/MS upon ion exchange column chromatography. The proteins identified were grouped into 12 different categories on the basis of functions and/or localization.

MT cytoskeletal proteins

Our analysis detected many MAPs previously shown to be biochemically associated with MTs. These included not only side-binding proteins (e.g. MAP1A/B, MAP2 and τ) but also plus-end-binding proteins (e.g. CLIP-115, CLIP-170 and EB1). However, we failed to identify several MAPs, such as MAP4, APC, NuMA and CENP-E. These MAPs may have been missed by MS because of an extremely low abundance in the brain or weak interaction with MTs (removed by washing). Furthermore, a minus-end-binding protein, γ-tubulin, was not identified. γ-Tubulin not only associates with centrosomes but also exists as a cytosolic form (Moudjou *et al.* 1996). The cytosolic form is shown to be capable of binding to taxol-stabilizing MTs. This binding of γ-tubulin to MTs is resistant to salt, ATP and GTP treatment. Thus, a possible explanation for the absence of γ-tubulin in our identified proteins is that γ-tubulin was co-sedimented with MTs but was not released from MTs with NaCl and ATP.

Other cytoskeletal proteins

We detected actin, intermediate filaments and septin cytoskeletal proteins. MTs, actin microfilaments and intermediate filaments are the three main cytoskeletal systems (Rodriguez *et al.* 2003; Chang & Goldman 2004). Although these systems are composed of distinctly different proteins, they are assumed to interact with each other. Septins are also regarded as cytoskeletal components that associate with the actin and MT cytoskeleton (Spiliotis & Nelson 2006). We identified several molecular linkers for mediating structural interactions of these cytoskeletal systems. MAP2 possesses both actin- and MT-binding sites and is regarded as a linker protein

© 2008 The Authors
Journal compilation © 2008 by the Molecular Biology Society of Japan/Blackwell Publishing Ltd.

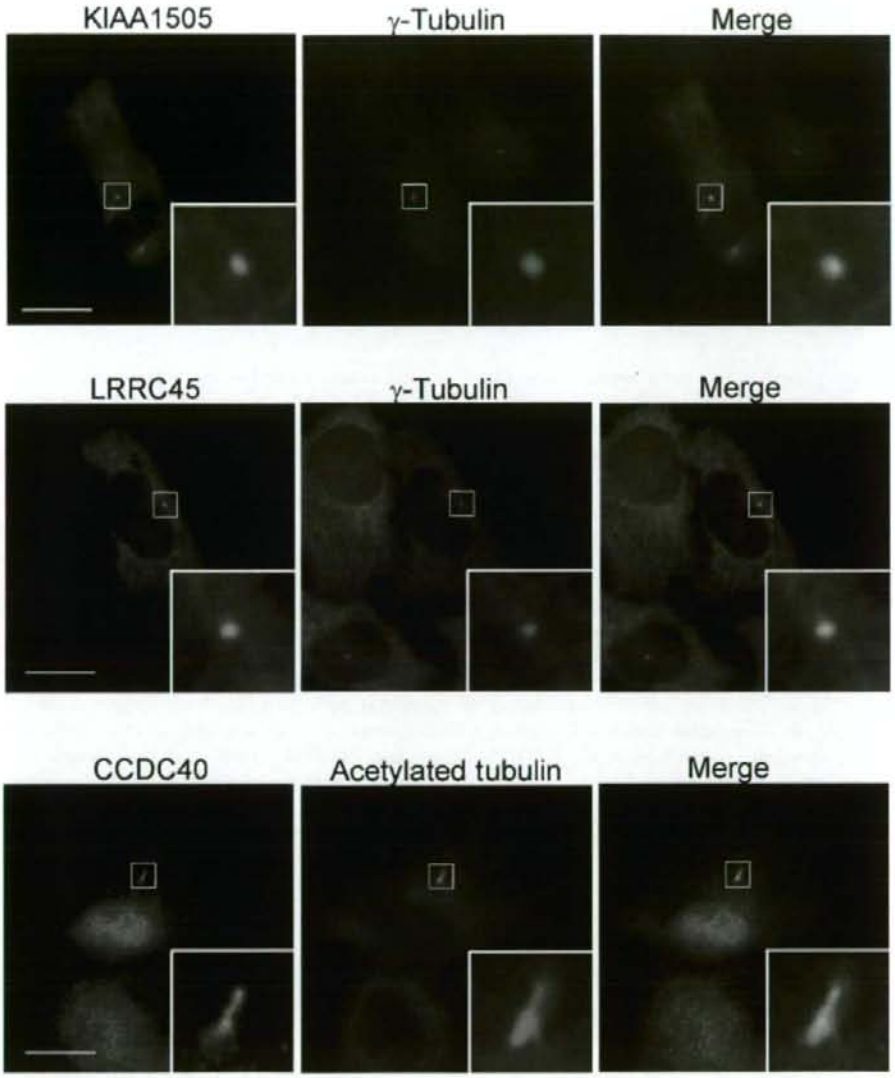

Figure 6 Localization of three uncharacterized proteins. EGFP-fusion proteins of KIAA1505, LRRC45 and CCDC40 were transiently expressed in RPE-1 cells. Cells were double stained with anti-EGFP Ab and anti-γ-tubulin Ab or anti-acetylated tubulin Ab. Samples were examined with a fluorescence microscopy. There was cytoplasmic or nuclear staining, but its significance is not clear. Insets, enlarged images of boxes. Scale bars, 10 μm.

between actin and MTs (Rodriguez *et al.* 2003). Intermediate filaments are assumed to be critical in mediating structural interactions between MTs and actin, functioning through plakins, a family of cytoskeletal cross-linkers. Plakins are large multidomain proteins that bind intermediate filaments and are essential for maintaining tissue integrity (Chang & Goldman 2004). Several plakins, including plectin, bullous pemphigoid antigen 1 and

© 2008 The Authors
Journal compilation © 2008 by the Molecular Biology Society of Japan/Blackwell Publishing Ltd.

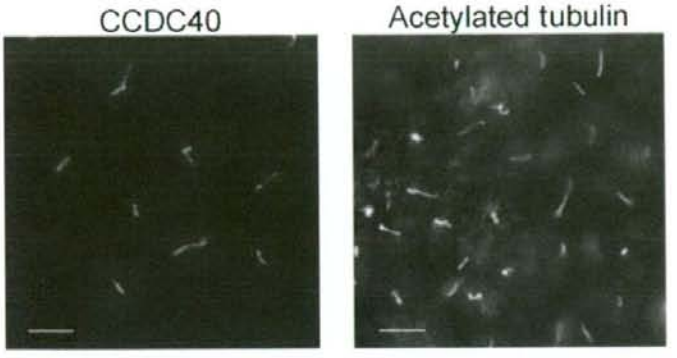

Figure 7 Localization of CCDC40 at cilia. MDCK cells were transfected with a recombinant retrovirus carrying Myc-tagged CCDC40. MDCK cells were grown for 7 days on Transwell filters. Cells were single stained with anti-Myc Ab or anti-acetylated tubulin Ab. The samples were examined with a fluorescence microscopy. Scale bars, 10 μm.

MT-actin cross-linking factor, also contain actin- and MT-binding sites. Identification of MAP2 and plakins, together with the actin and intermediate filament proteins, suggests that the three cytoskeletal systems are interlinked by these linker proteins.

Centrosomal proteins

chTOG, which we identified, is an MAP predominantly localized at centrosomes (Kinoshita *et al.* 2002), although this protein was classified here into MT cytoskeletal proteins. Identification of this MAP indicates that our method is useful for detecting low abundant MAPs localized at MT-based structures. Several other components of centrosomes were also identified. It is not clear how they were co-sedimented with MTs, but chTOG is known to interact with centrosomal proteins (Ohkura *et al.* 2001). chTOG may mediate interaction of these centrosomal proteins with MTs.

Chaperones

We identified several chaperones. HSP70s were originally characterized as MAPs before they were identified as molecular chaperons (Liang & MacRae 1997). HSP90 was also shown to associate with MTs in cultured cells. Furthermore, it was shown that the chaperons directly associate with τ, an MAP, and increase the association of τ with MTs (Dou *et al.* 2003). On the basis of these observations, it is proposed that molecular chaperones have roles in MT organization (Liang & MacRae 1997). Our results are consistent with this proposal.

Other proteins

MTs not only play a role in sister chromatid segregation, but also serve as major tracks for the intracellular transport of ribosomes, mitochondria, membrane vesicles and RNA granules. RNA granules transport a subset of mRNAs to axons or dendrites through RNA-binding proteins, referred to as heterogeneous nuclear ribonucleoproteins (hnRNPs), along MTs (Carson & Barbarese 2005; Anderson & Kedersha 2006). MTs are furthermore involved in the migration and positioning of the nucleus and Golgi, although it is poorly understood how the nucleus and Golgi interact with MTs (Barr & Egerer 2005; Starr 2007). Several proteins localized at these organelles were consistently identified, suggesting that these proteins may directly or indirectly interact with MTs. In addition, we identified many proteins with diverse cellular functions and/or localization. Similar multiplicity has also been reported in MS screening of MT-based structures, spindles and cilia (Ostrowski *et al.* 2002; Sauer *et al.* 2005). Consistent with these previous reports, our results suggest that many more proteins are involved in MT-based functions and structures than previously assumed.

A major concern is nonspecific contamination by proteins unrelated to MTs. Such contamination would contribute artifactually to the observed multiplicity of MT co-sedimented proteins. However, we identified hnRNP A2, a component of RNA granules, which is shown to bind to chTOG and proposed to mediate the association of hnRNP A2-positive granules with MTs (Kosturko *et al.* 2005). Furthermore, KARP-1-binding protein 2/KAB1/Cep170 was originally identified as a binding partner of KARP-1, a DNA-binding protein (Do *et al.* 2003), but it has been found to associate with the mature mother centrioles and spindle MTs during mitosis (Guarguaglini *et al.* 2005). It is, therefore, plausible that at least some of presumptive impurities actually reflect a specific association with MTs or a role as MAPs.

Of 42 uncharacterized proteins, three proteins with coiled-coil domains (KIAA1505, LRRC45 and CCDC40) were novel components of centrosomes and cilia. In

© 2008 The Authors
Journal compilation © 2008 by the Molecular Biology Society of Japan/Blackwell Publishing Ltd.

addition, we have found another novel centrosomal protein (Q9NXG0) and named it centlein (Makino *et al.* 2008). This protein also contains coiled-coil domains. Centrosomes are known to be made up of numerous proteins with coiled-coil domains (Doxsey *et al.* 2005). Increasing evidence indicates that this molecular structure may be well designed for the organization of protein complexes, such as MT-based structures. Of the uncharacterized proteins, those with coiled-coil domains are highly expected to be components of MT-based structures.

Compared to previous MS analyses of isolated MT-based structures, such as centrosomes, cilia and mitotic spindles (Ostrowski *et al.* 2002; Andersen *et al.* 2003; Keller *et al.* 2005; Pazour *et al.* 2005; Sauer *et al.* 2005; Nousiainen *et al.* 2006; Reinders *et al.* 2006), our method is characterized by anion exchange column chromatography used to enrich low abundant proteins. It is likely that this chromatography contributes to the identification of novel components of centrosomes and cilia, which have not been previously identified. In conclusion, our present method is useful for identifying low abundant novel MAPs and components of MT-based structures. Our analysis provides an extensive list of potential candidates for future analysis. It is important to follow up the proteomics approach with more focused experiments to examine whether these candidate proteins show a specific association with MTs and/or MT-based structures and, if so, what their physiological functions are?

Experimental procedures

Preparation of MTs

Tubulin was purified from fresh porcine brains by three cycles of polymerization and depolymerizaiton (Shelanski *et al.* 1973) followed by DEAE-Sephadex column chromatography (Williams & Lee 1982). Purified tubulin was stored at −80 °C until use. MTs were prepared by incubation of purified tubulin (4 mg/mL) for 20 min at 37 °C in polymerization buffer (80 mM PIPES–NaOH, pH 6.8, 1 mM $MgCl_2$, 1 mM EGTA, 1 mM GTP and 10% glycerol) (Yamamoto *et al.* 2002; Uezu *et al.* 2007). After the incubation, taxol was added to give a final concentration of 15 μM.

Preparation and resolution of MT co-sedimented proteins

All the purification procedures were carried out at 0–4 °C. Twenty rat brains were homogenized in 100 mL of buffer A (50 mM HEPES–NaOH, pH 7.5, 5 mM EGTA, 2 mM EDTA, 1 mM DTT, 50 mM NaF, 1 mM Na_3VO_4, 0.1% Triton X-100, 1 mM PMSF, 10 μg/mL of leupeptin and 1 μg/mL of pepstatin A). The homogenate was subjected to ultracentrifugation at 100 000 *g* for 1 h. The supernatant and pellet were employed as the soluble and insoluble fractions, respectively. MT co-sedimented proteins from the soluble fraction were prepared as follows: $MgCl_2$, GTP and taxol were added to the soluble fraction to give final concentrations of 4 mM, 1 mM and 20 μM, respectively. The sample was then incubated with 1 mg/mL of MTs for 3 h. The mixture was placed over a 20-mL cushion of 10% sucrose in HEM buffer (50 mM HEPES–NaOH, pH 7.5, 1 mM EGTA, 1 mM $MgCl_2$, 50 mM NaF, and 1 mM Na_3VO_4, 1 mM GTP and 20 μM taxol), followed by ultracentrifugation at 100 000 *g* for 30 min. The pellet (P1) was rinsed with HEM buffer and then homogenized in 20 mL of HEM buffer containing 50 mM NaCl, followed by ultracentrifugation at 100 000 *g* for 30 min. The pellet (P2) was rinsed with HEM buffer and then homogenized in 20 mL of HEM buffer containing 0.5 M NaCl and 0.1 mM ATP to dissociate co-sedimented proteins from MTs, followed by ultracentrifugation at 100 000 *g* for 30 min. The supernatant (S3, 24 mg of protein) was collected and used as MT co-sedimented proteins from the soluble fraction.

The extract fraction was prepared as follows: the insoluble fraction was re-homogenized in 20 mL of buffer A containing 1.0 M NaCl. The homogenate was mildly stirred for 30 min and centrifuged at 100 000 *g* for 1 h. The supernatant was diluted with 120 mL of buffer A, followed by ultracentrifugation at 100 000 *g* for 1 h. The supernatant was collected and the concentration of NaCl was examined by measuring the conductivity. The sample was further diluted with buffer A and brought to a final concentration of 100 mM NaCl. This sample was employed as the extract fraction. The extract fraction was then subjected to MT co-sedimentation in the same manner as described above.

MT co-sedimented proteins from the soluble and extract fractions (10 mg of protein each) were separately subjected to precipitation by a chloroform–methanol–water system (Pohl 1990) and dissolved in 5 mL of buffer B (40 mM Tris–HCl, pH 8.0, 1 mM EDTA, 1 mM DTT, 0.6% CHAPS and 4 M urea). The sample was applied to a BioAssist Q column (4.6 × 50 mm; Tosoh, Tokyo, Japan) equilibrated with buffer B. The column was washed with 20 mL of buffer B, and elution was performed with a 12.5-mL linear gradient (0–0.25 M) of NaCl in buffer B and a subsequent 6.25-mL linear gradient (0.25–0.5 M) of NaCl in buffer B, followed by 6.25 mL of 1 M NaCl in buffer B. Fractions of 0.5 mL each were collected.

Identification by MS/MS analysis

Each fraction of BioAssist Q column chromatography was subjected to SDS-PAGE (10% polyacrylamide gel), followed by protein staining with silver (Shevchenko *et al.* 1996). Each protein band was excised and digested with trypsin (Promega, Madison, WI). After destaining with 100 μL of 10 mM potassium ferricyanide and 50 mM sodium thiosulfate (Gharahdaghi *et al.* 1999), the gel pieces were dried and swollen in digestion buffer [50 mM ammonium bicarbonate, 10% acetonitrile (ACN) and 10 ng/μL trypsin], and incubated at 37 °C for 16 h. Peptides were extracted by 30% and 80% ACN then concentrated in a vacuum centrifuge. Dried samples were dissolved in 15 μL of 0.1% trifluoroacetic acid (TFA) then desalted by Zip tips C18 (Millipore, Bedford, MA)

© 2008 The Authors
Journal compilation © 2008 by the Molecular Biology Society of Japan/Blackwell Publishing Ltd.

and peptides were mixed with matrix solution (10 mg/mL a-cyano-4-hydroxycinnamic acid in 50% ACN and 0.1% TFA) and crystallized onto the 576-well target plate. Matrix-laser desorption/ionization-time of flight (TOF) and tandem TOF data were acquired in batch mode using an ABI4700 Proteomics Analyzer (Applied Biosystems. Foster City, CA). MS reflector positive ion mode with automated acquisition of 800–4000 m/z range was used with 1000 shots per spectrum. A maximum of 10 peaks were selected per spot, with a minimum signal : noise ratio of 10 and a cluster area of 200. Precursor ions were submitted for MS/MS, where a positive ion mode with a collision induced-dissociation cell and 1kV collision energy were used, and 5000 shots were accumulated per spectrum. Database searching was performed with the GPS EXPLORER SOFTWARE (Applied Biosystems) utilizing Mascot (v1.9) at the search engine (Matrix Science Ltd., London, UK) allowing ±0.3 Da as the parent tolerance and ±0.1 Da as the fragment ion tolerance. Combined peak lists were searched against the non-redundant Swiss-Prot database, and the oxidation of methionine and one possible missed cleave site was selected as a variable modification. Peptides were considered identified if their Mascot score was at or over the 95% confidence limit; meaning that the fragmentation data is of sufficient quality as to have a > 95% probability of being assigned to the proper peptide sequence. Proteins were considered identified if at least one peptide matched to it with a significant Mascot score.

Molecular cloning

Q8N2T9 was obtained from the Kazusa DNA Research Institute. Q8IYE0 was purchased from Invitrogen (Carlsbad, CA) (MGC clone, 5273288). Q8BI79 (RikenB930008102) was purchased from DNAFORM (Yokohama, Japan). The following cDNAs were obtained by PCR : Q9CRC8, (primers) 5′-CTG CAG CTT CTG GAC CTA GGA CTT TG-3′ and 5′-ATG ACA AGG GTT ATA AAG CAA CTC CAT G-3′, (template) HeLa cell cDNA; Q96MC5, (primers) 5′-GAT CAG CGA TGG AAT TAA AGC AAT C-3′ and 5′-GAC TCC CTA CTG CTA CAC TCT GTA CAG-3′, (template) HeLa cell cDNA; and Q8CIM1, (primers) 5′-GAA TTC ATG GAG GAG TTC CGG CGC TCC TAC-3′ and 5′-GTC GAC TCA TTT AGG GGG ATC CAA GGC TCT C-3′, (template) mouse brain cDNA. These cDNAs were cloned into pEGFP-C1 (Clontech. Mountain View, CA) and pMXII-Myc (Ono *et al.* 2000).

Cell culture, transfection and immunofluorescence microscopy

RPE-1 and MDCK cells were maintained at 37 °C in Dulbecco's modified Eagle's medium supplemented with 10% fetal calf serum. Transfection was performed using FuGene6 (Roche Diagnostics, Basel, Switzerland) transfection reagent according to the manufacturer's protocol. For cilia immunostaining in RPE-1 cells, cells were cultured in medium with 0.25% serum for 48 h (Gromley *et al.* 2003). For cilia immunostaining in MDCK cells, a recombinant retrovirus carrying Myc-CDCC40 cDNA was prepared with pMXII-Myc (Nishimura *et al.* 2002). MDCK cells were infected with the recombinant retrovirus and cultured for 1 day. After the medium was changed, the cells were grown for 7 days post-confluence on 10 mm Transwell filters as described (Fan *et al.* 2004).

The following antibodies (Abs) were purchased from commercial sources: mouse anti-Myc monoclonal Ab (9E10) (American Type Culture Collection, Manassas, VA); mouse anti-acetylated tubulin (clone 6-11B-1) and mouse anti-γ-tubulin monoclonal Abs (Sigma-Aldrich, Seelze, Germany); rabbit anti-EGFP polyclonal Ab (MBL Co., Nagoya, Japan); and secondary Abs conjugated with Alexa Fluor 488 and 594 (Invitrogen). For immunofluorescence microscopy, cells were fixed in 100% methanol at −20 °C for 3 min. After blocking with 1% bovine serum albumin for 1 h at room temperature, the samples were incubated with primary Abs for 1 h, followed by incubation with second Abs for 30 min. The samples were viewed with a florescence microscope (Olympus, BX51).

Other procedures

Protein concentrations were determined with bovine serum albumin as a reference protein (Bradford 1976). SDS-PAGE was done as described (Laemmli 1970).

Acknowledgements

This study was supported by grants-in-aids for Scientific Research on Priority Areas from the Ministry of Education, Culture, Sports, Science, and Technology of Japan.

References

Andersen, J.S., Wilkinson, C.J., Mayor, T., Mortensen, P., Nigg, E.A. & Mann, M. (2003) Proteomic characterization of the human centrosomes by protein correlation profiling. *Nature* **426**, 570–574.

Anderson, P. & Kedersha, N. (2006) RNA granule. *J. Cell Biol.* **172**, 803–808.

Barr, F.A. & Egerer, J. (2005) Golgi positioning: are we looking at the right MAP? *J. Cell Biol.* **168**, 993–998.

Bettencourt-Dias, M. & Glover, D.M. (2007) Centrosome biogenesis and function: centrosomics brings new understanding. *Nat. Rev. Mol. Cell Biol.* **8**, 451–463.

Bradford, M.M. (1976) A rapid and sensitive method for the quantitation of microgram quantities of protein utilizing the principle of protein-dye binding. *Anal. Biochem.* **72**, 248–254.

Carson, J.H. & Barbarese, E. (2005) Systems analysis of RNA trafficking in neural cells. *Biol. Cell* **97**, 51–62.

Cassimeris, L. & Spittle, C. (2001) Regulation of microtubule-associated proteins. *Int. Rev. Cytol.* **210**, 163–226.

Chang, L. & Goldman, R.D. (2004) Intermediate filaments mediate cytoskeletal crosstalk. *Nat Rev. Mol. Cell Biol.* **5**, 601–613.

Do, E., Taira, E., Irie, Y., Gan, Y., Tanaka, H., Kuo, C.H. & Miki, N. (2003) Molecular cloning and characterization of rKAB1, which interacts with KARP-1, localizes in the nucleus and protects cells against oxidative death. *Mol. Cell. Biochem.* **248**, 77–83.

© 2008 The Authors
Journal compilation © 2008 by the Molecular Biology Society of Japan/Blackwell Publishing Ltd.

Dou, F., Netzer W.J., Tanemura, K., Li, F., Hartl, F.U., Takashima, A., Gouras, G.K., Greengard, P. & Xu, H. (2003) Chaperones increase association of τ protein with microtubules. *Proc. Natl. Acad. Sci. USA* **100**, 721–726.

Doxsey, S., McCollum, D. & Theurkauf, W. (2005) Centrosomes in cellular regulation. Annu. *Rev. Cell Dev. Biol.* **21**, 411–434.

Fan, S., Hurd, T.W., Liu, C-J., Straight, S.W., Weimbs, T., Hurd, E.A., Domino, S.E. & Margolis, B. (2004) Polarity proteins control ciliogenesis via kinesin motor interactions. *Curr. Biol.* **14**, 1451–1461.

Gharahdaghi, F., Weinberg, C.R., Meagher, D.A., Imai, B.S. & Mische, S.M. (1999) Mass spectrometric identification of proteins from silver-stained polyacrylamide gel: a method for the removal of silver ions to enhance sensitivity. *Electrophoresis* **20**, 601–605.

Gromley, A., Jurczyk, A., Sillibourne, J., Halilovic, E., Mogensen, M., Groisman, I., Blomberg, M. & Doxsey, S. (2003) A novel human protein of the maternal centriole is required for the final stages of cytokinesis and entry into S phase. *J. Cell Biol.* **161**, 535–545.

Guarguaglini, G., Duncan, P.I., Stierhof, Y.D., Holmström, T., Duensing, S. & Nigg, E.A. (2005) The forkhead-associated domain protein Cep170 interacts with Polo-like kinase 1 and serves as a marker for mature centrioles. *Mol. Biol. Cell* **16**, 1095–1107.

Keller, L.C., Romijn, E.P., Zamora, I., Yates, J.R. 3rd & Marshall, W.F. (2005) Proteomic analysis of isolated chlamydomonas centrioles reveals orthologs of ciliary-disease genes. *Curr. Biol.* **15**, 1090–1098.

Kellogg, D.R., Field, C.M. & Alberts, B.M. (1989) Identification of microtubule-associated proteins in the centrosome, spindle, and kinetochore of the early *Drosophila* embryo. *J. Cell Biol.* **109**, 2977–2991.

Kinoshita, K., Habermann, B. & Hyman, A.A. (2002) XMAP215: a key component of the dynamic microtubule cytoskeleton. *Trends Cell Biol.* **12**, 267–273.

Kirschner, M. & Mitchison, T. (1986) Beyond self-assembly: from microtubules to morphognesis. *Cell* **45**, 329–342.

Kosturko, L.D., Maggipinto, M.J., D'Sa, C., Carson, J.H. & Barbarese, E. (2005) The microtubule-associated protein tumor overexpressed gene binds to the RNA trafficking protein heterogeneous nuclear ribonucleoprotein A2. *Mol. Biol. Cell* **16**, 1938–1947.

Laemmli, U.K. (1970) Cleavage of structural proteins during the assembly of the head of bacteriophage T4. *Nature* **227**, 680–685.

Liang, P. & MacRae, T.H. (1997) Molecular chaperones and the cytoskeleton. *J. Cell Sci.* **110**, 1431–1440.

Linck, R.W. & Stephens, R.E. (2007) Functional protofilament numbering of ciliary, flagellar, and centriolar microtubules. *Cell Motil. Cytoskeleton* **64**, 489–495.

Makino, K., Umeda, K., Uezu, A, Hiragami, Y., Sakamoto, T., Ihn, H. & Nakanishi, H. (2008) Identification and characterization of the novel centrosomal protein centlein. *Biochem. Biophys. Res. Commun.* **366**, 958–962.

Moudjou, M., Bordes, N., Paintrand, M. & Bournes, M. (1996) γ-Tubulin in mammalian cells: the centrosomal and cytosolic forms. *J. Cell Sci.* **109**, 875–887.

Nishimura, M., Kakizaki, M., Ono, Y., Morimoto, K., Takeuchi, M., Inoue, Y., Imai, T. & Takai, Y. (2002) JEAP, a novel component of tight junctions in exocrine cells. *J. Biol. Chem.* **227**, 5583–5587.

Nousiainen, M., Silljé, H.H., Sauer, G., Nigg, E.A. & Körner, R. (2006) Phosphoproteome analysis of the human mitotic spindle. *Proc. Natl. Acad. Sci. USA* **103**, 5391–5396.

Ohkura, H., Carcia, M.A. & Toda, T. (2001) Dis1/TOG universal microtubule adaptors-one MAP for all. *J. Cell Sci.* **114**, 3805–3812.

Olmstead, J.B. (1986) Microtubule-associated proteins. *Ann. Rev. Cell Biol.* **2**, 421–457.

Ono, Y., Nakanishi, H., Nishimura, M., Kakizaki, M., Takahashi, K., Miyahara, M., Satoh-Horikawa, K., Mandai, K. & Takai, Y. (2000) Two actions of frabin: direct activation of Cdc42 and indirect activation of Rac. *Oncogene* **19**, 3050–3058.

Ostrowski, L.E., Blackburn, K., Radde, K.M., Moyer, M.B., Schlatzer, D.M., Moseley, A. & Boucher, R.C. (2002) A proteomic analysis of human cilia: identification of novel components. *Mol. Cell. Proteomics* **1**, 451–465.

Pazour, G.J., Agrin, N., Leszyk, J. & Witman, G.B. (2005) Proteomic analysis of a eukaryotic cilium. *J. Cell Biol.* **170**, 103–113.

Pipemo, G. & Fuller, M.T. (1985) Monoclonal antibodies specific for an acetylated form of α-tubulin recognize the antigen in cilia and flagella from a variety of organisms. *J. Cell Biol.* **101**, 2085–2094.

Pohl, T. (1990) Concentration of proteins and removal of solutes. *Methods Enzymol.* **182**, 68–83.

Reinders, Y., Schulz, I., Gräf, R. & Sickmann, A. (2006) Identification of novel centrosomal proteins in *Dictyostelium discoideum* by comparative proteomic approaches. *J. Proteome Res.* **5**, 589–598.

Richard, J.E. & Kreis, T.E. (1990) Identification of a novel nucleotide-sensitive microtubule-binding protein in HeLa cells. *J. Cell Biol.* **110**, 1623–1633.

Rodriguez, O.C., Schaefer, A.W., Mandato, C.A., Forscher, P., Bement, W.M. & Waterman-Storer, C.M. (2003) Conserved microtubule–actin interactions in cell movement and morphogenesis. *Nat. Cell Biol.* **7**, 599–609.

Rogers, S.L. & Gelfand, V.I. (2000) Membrane trafficking, organelle transport, and the cytoskeleton. *Curr. Opin. Cell Biol.* **12**, 57–62.

Satir, P. & Christensen, S.T. (2007) Overview of structure and function of mammalian cilia. *Annu. Rev. Physiol.* **69**, 377–400.

Sauer, G., Körner, R., Hanisch, A., Ries, A., Nigg, E.A. & Silljé, H.H. (2005) Proteome analysis of the human spindle. *Mol. Cell. Proteomics* **4**, 35–43.

Shelanski, M.L., Gaskin, F. & Cantor, C.R. (1973) Microtubule assembly in the absence of added nucleotides. *Proc. Natl. Acad. Sci. USA* **70**, 765–768.

Shevchenko, A., Wilm, M., Vorm, O. & Mann, M. (1996) Mass spectrometric sequencing of proteins from silver-stained polyacrylamide gels. *Anal. Chem.* **68**, 850–858.

© 2008 The Authors
Journal compilation © 2008 by the Molecular Biology Society of Japan/Blackwell Publishing Ltd.

Siegrist, S.E. & Doe, C.Q. (2007) Microtubule-induced cortical cell polarity. *Genes Dev.* **21**, 483–496.

Spiliotis, E.T. & Nelson, W.J. (2006) Here comes the septins: novel polymers that coordinate intracellular functions and organization. *J. Cell Sci.* **119**, 4–10.

Starr, D.A. (2007) Communication between the cytoskeleton and the nuclear envelope to position the nucleus. *Mol. Biosys.* **3**, 583–589.

Uezu, A., Horiuchi, A., Kanda, K., Kikuchi, N., Umeda, K., Tsujita, K., Suetsugu, S., Araki, N., Yamamoto, H., Takenawa, T. & Nakanishi, H. (2007) SGIP1α is an endocytic protein that directly interacts with phospholipids and Eps15. *J. Biol. Chem.* **282**, 26481–26489.

Vallee, R.B., Bloom, G.S. & Theurkauf, W.E. (1984) Microtubule-associated proteins: subunits of the cytomatrix. *J. Cell Biol.* **99**, 38s–44s.

Wemmer, K.A. & Marshall, W.F. (2004) Flagella motility: all put together. *Curr. Biol.* **14**, R992–R993.

Williams, R.C. Jr. & Lee, J.C. (1982) Preparation of tubulin from brain. *Methods Enzymol.* **85**, 376–385.

Yamamoto, H., Yamauchi, E., Taniguchi, H., Ono, T. & Miyamoto, E. (2002) Phosphorylation of microtubule-associated protein τ by Ca2/calmodulin-dependent protein kinase II in its tubulin binding sites. *Arch. Biochem. Biophys.* **408**, 255–262.

Received: 20 November 2007
Accepted: 19 December 2007

© 2008 The Authors
Journal compilation © 2008 by the Molecular Biology Society of Japan/Blackwell Publishing Ltd.

Oncogene (2008) 27, 4305–4314
© 2008 Macmillan Publishers Limited All rights reserved 0950-9232/08 $30.00
www.nature.com/onc

ORIGINAL ARTICLE

Aurora A overexpression induces cellular senescence in mammary gland hyperplastic tumors developed in p53-deficient mice

D Zhang[1,6], T Shimizu[1,7], N Araki[1], T Hirota[2], M Yoshie[3], K Ogawa[3], N Nakagata[4], M Takeya[5] and H Saya[1,7]

[1]Department of Tumor Genetics and Biology, Graduate School of Medical Sciences, Kumamoto University, Kumamoto, Japan; [2]Department of Experimental Pathology, Cancer Institute of Japanese Foundation for Cancer Research, Tokyo, Japan; [3]Department of Pathology, Asahikawa Medical College, Asahikawa, Japan; [4]Division of Reproductive Engineering, Center for Animal Resources and Development, Kumamoto University, Kumamoto, Japan and [5]Department of Cell Pathology, Graduate School of Medical Sciences, Kumamoto University, Kumamoto, Japan

Aurora A mitotic kinase is frequently overexpressed in various human cancers and is widely considered to be an oncoprotein. However, the cellular contexts in which Aurora A induces malignancy *in vivo* are still unclear. We previously reported a mouse model in which overexpression of human Aurora A in the mammary gland leads to small hyperplastic changes but not malignancy because of the induction of p53-dependent apoptosis. To study the additional factors required for Aurora A-associated tumorigenesis, we generated a new Aurora A overexpression mouse model that lacks p53. We present evidence here that Aurora A overexpression in primary mouse embryonic fibroblasts (MEFs) that lack p53 overrides postmitotic checkpoint and leads to the formation of multinucleated polyploid cells. Induction of Aurora A overexpression in the mammary glands of p53-deficient mice resulted in development of precancerous lesions that were histologically similar to atypical ductal hyperplasia in human mammary tissue and showed increased cellular senescence and p16 expression. We further observed DNA damage in p53-deficient primary MEFs after Aurora A overexpression. Our results suggest that Aurora A overexpression in mammary glands is insufficient for the development of malignant tumors in p53-deficient mice because of the induction of cellular senescence. Both p53 and p16 are critical in preventing mammary gland tumorigenesis in the Aurora A overexpression mouse model.

Oncogene (2008) **27**, 4305–4314; doi:10.1038/onc.2008.76; published online 31 March 2008

Keywords: Aurora A; polyploidy; apoptosis; senescence; p16; DNA damage

Introduction

Mitotic kinases such as cyclin-dependent kinase 1, polo-like kinases, NIMA-related kinases, WARTS/LATS1-related kinases and Aurora/Ipl1-related kinases have been widely reported to play crucial roles in regulating cell division and checkpoint functions. Dysfunction of some mitotic kinases leads to chromosome rearrangements and aneuploidy, which are hallmarks of many human cancers, indicating that mitotic kinases are important for maintaining genomic integrity (Nigg, 2001). Aurora A serine/threonine mitotic kinase has crucial roles in various mitotic events such as centrosome maturation and separation, mitotic entry, bipolar spindle assembly, chromosome alignment and cytokinesis (Meraldi *et al.*, 2002; Hirota *et al.*, 2003; Kunitoku *et al.*, 2003; Marumoto *et al.*, 2003, 2005; Giet *et al.*, 2005).

Many reports have presented evidence that Aurora A functions as an oncogene product. The human *Aurora A* gene is located at chromosome 20q13.2, a region frequently amplified in various human cancers (Kallioniemi *et al.*, 1994). Human *Aurora A* gene amplification has been found in several human tumor cell types, including primary breast and colorectal cancers (Sen *et al.*, 1997; Bischoff *et al.*, 1998; Zhou *et al.*, 1998). Aurora A mRNA and protein are frequently overexpressed in a range of cancer types, including breast, colorectal, gastric, ovarian and hepatocellular carcinoma (Tanaka *et al.*, 1999; Sakakura *et al.*, 2001; Gritsko *et al.*, 2003; Jeng *et al.*, 2004). Aurora A overexpression has been linked with centrosome amplification, aneuploidy and chromosome instability (Zhou *et al.*, 1998; Cahill *et al.*, 1999; Meraldi *et al.*, 2002). Furthermore, ectopic overexpression of Aurora A efficiently transforms immortalized rodent fibroblasts (Bischoff *et al.*, 1998; Zhou *et al.*, 1998).

Correspondence: Dr H Saya, Division of Gene Regulation, Institute for Advanced Medical Research, Keio University School of Medicine, 35 Shinano-machi, Shinjuku-ku, Tokyo 160-8582, Japan.
E-mail: hsaya@a5.keio.jp
[6]Current address: Breast Cancer Translational Research Laboratory, Department of Stem Cell Transplantation and Cellular Therapy, The University of Texas MD Anderson Cancer Center, Houston, TX, USA.
[7]Current address: Division of Gene Regulation, Institute for Advanced Medical Research, Keio University School of Medicine, Tokyo, Japan.
Received 18 April 2007; revised 30 January 2008; accepted 20 February 2008; published online 31 March 2008

Breast cancer is one of the most common cancers and a leading cause of cancer death among women in the Western hemisphere (Howe *et al.*, 2001). Evidence of *Aurora A* gene amplification and Aurora A overexpression in human breast cancer suggests that Aurora A may be involved in the pathogenesis of that cancer. Increases in endogenous Aurora A expression and centrosome number were also noted in a carcinogen-induced rat mammary tumor model, suggesting that Aurora A has a critical role during mammary tumor development and progression (Goepfert *et al.*, 2002). However, the precise cellular conditions under which Aurora A expression promotes mammary tumorigenesis remain unclear.

We previously used the Cre-loxP system to develop a *CAG-CAT-Aurora A;Wap-Cre* transgenic mouse model that conditionally overexpresses Aurora A in adult mammary glands (Zhang *et al.*, 2004). Elevated Aurora A expression in these mice induces failure of cytokinesis, leading to the formation of binucleated and hyperploid cells in the mammary epithelium. Although small papillary hyperplasias were found in mammary glands overexpressing Aurora A, no tumorous lesions were identified. Given that Aurora A overexpression induced p53-dependent apoptosis in our model, we hypothesized that additional factors such as p53 inactivation may be required for the tumorigenesis of Aurora A-overexpressing mammary epithelium. To test this hypothesis, we generated *CAG-CAT-Aurora A;Wap-Cre* transgenic mice carrying heterozygous or null alleles for p53 and found that Aurora A overexpression can override the postmitotic checkpoint and lead to the formation of multinucleated polyploid cells in p53-deficient primary mouse embryonic fibroblasts (MEFs). These mice frequently developed tumorous hyperplasia in mammary glands, but lesions were considered nonmalignant and precancerous. Aurora A-expressing p53-deficient mammary gland cells also expressed high levels of senescence markers and $p16^{INK4a}$ (p16). Our findings suggest that p16 plays critical roles for preventing mammary gland malignancy in our p53-deficient Aurora A overexpression mouse model by inducing cellular senescence.

Results

Wap-Cre-mediated Aurora A overexpression in the mammary glands of p53-deficient mice

We previously reported generating *CAG-CAT-Aurora A;Wap-Cre* double-transgenic mice that conditionally overexpress human Aurora A in adult mammary glands by using the Cre-loxP recombination system under the control of the Wap promoter (Zhang *et al.*, 2004). Even though Aurora A overexpression induced the formation of binucleated cells and papillary hyperplastic changes in mammary tissues, no malignant tumors were found because Aurora A had induced p53-dependent apoptosis. To further investigate the involvement of p53 in Aurora A-associated tumorigenesis, we generated *CAG-CAT-Aurora A;Wap-Cre* transgenic mice carrying heterozygous or null alleles for p53 (*CAG-CAT-Aurora A;Wap-Cre;p53+/−* mice and *CAG-CAT-Aurora A;Wap-Cre;p53−/−* mice, respectively). Immunohistochemical analyses confirmed the successful Wap-Cre-mediated human Aurora A overexpression in the mammary glands of both the p53-heterozygous and p53-null mice. Aurora A overexpression was not detected in control *CAG-CAT-Aurora A;p53+/−* or *CAG-CAT-Aurora A;p53−/−* transgenic mice (Supplementary Figure S1).

Aurora A overexpression leads to formation of multinucleated polyploid cells in p53-null primary MEFs

We previously showed that induction of Aurora A overexpression in p53-wild-type (wt; +/+) mice resulted in failure of cytokinesis, leading to significantly increased numbers of mammary gland cells with two nuclei (Zhang *et al.*, 2004). To investigate the function of Aurora A in p53-deficient cells, we established primary MEFs from *CAG-CAT-Aurora A;p53+/+* and *CAG-CAT-Aurora A;p53−/−* transgenic mice and induced Aurora A overexpression in those MEFs *in vitro* by infection with AxCANCre (Kanegae *et al.*, 1995), an adenovirus that encodes the Cre enzyme (Figure 1a). Cre-mediated Aurora A overexpression significantly increased the percentage of cells containing more than three nuclei in *CAG-CAT-Aurora A;p53−/−* MEFs but not in *CAG-CAT-Aurora A;p53+/+* MEFs (Figures 1b and c). Induction of multinucleated cells by Aurora A expression was further confirmed *in vivo*. Cells having three or more than three nuclei were frequently detected in mammary glands of *p53−/−* mice, but rarely found in those of *p53+/+* mice (Supplementary Figure S2).

To determine whether those multinucleated polyploid cells could undergo further DNA synthesis, we used a bromodeoxyuridine (BrdU)-incorporation assay and found that the percentage of BrdU-positive polyploid cells was markedly increased when Aurora A was overexpressed in *p53−/−* MEFs ($13.6 \pm 1.52\%$), but only a small fraction of the polyploid cells were BrdU positive in *p53+/+* MEFs ($3.5 \pm 0.18\%$) (Figure 1d). These findings demonstrate that p53 deficiency allows further DNA synthesis in postmitotic polyploid MEFs produced by Aurora A overexpression. Therefore, the percentages of cells containing $>4N$ DNA content ($>4N$ DNA) (hyperploid cells and aneuploid cells) are significantly increased in Aurora A-overexpressing *p53−/−* MEFs by comparison to the *p53+/+* MEFs. Markedly increased number of centrosomes and abnormal spindle formation after Aurora A overexpression were also found in *p53−/−* MEFs compared with *p53+/+* MEFs (Supplementary Figure S3). These findings indicate that Aurora A overexpression on a p53-deficient background leads to the formation of hyperploid cells and aneuploid cells with aberrant cell division.

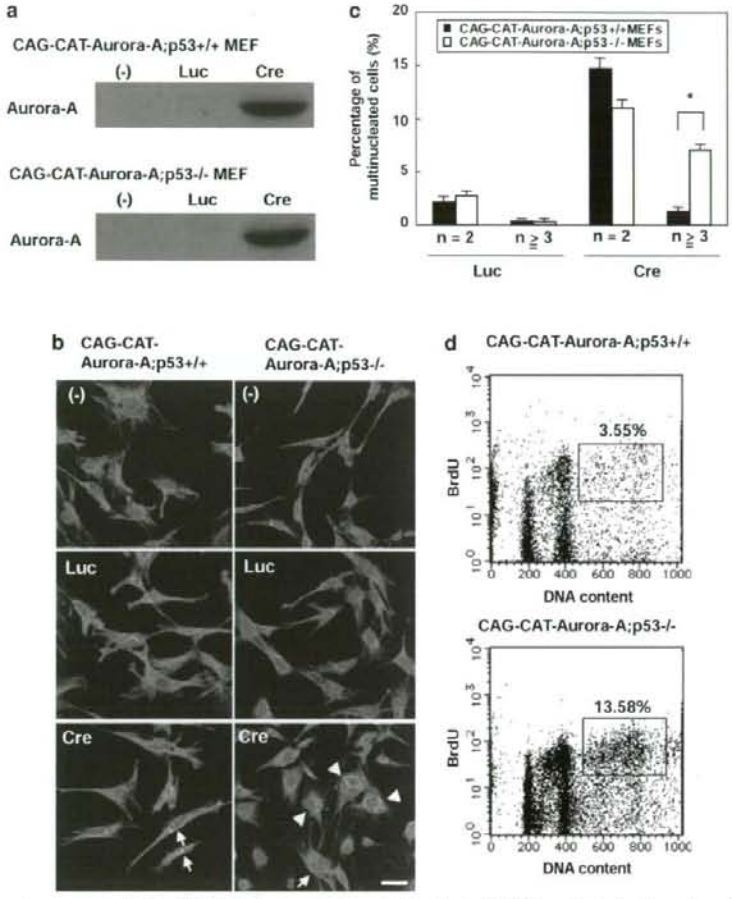

Figure 1 Aurora A overexpression in p53-deficient mouse embryonic fibroblasts (MEFs) results in the formation of multinucleated polyploid cells. (**a**) Primary MEFs from *CAG-CAT-Aurora A;p53+/+* mice (upper panel) and *CAG-CAT-Aurora A;p53−/−* mice (lower panel) were infected with adenoviral luciferase (Luc) or AxCANCre (Cre) virus (which induces Aurora A expression). Western blotting confirmed that Aurora A overexpression appeared 24 h after Cre infection. (−), uninfected. (**b**) Primary MEFs from *CAG-CAT-Aurora A;p53+/+* and *CAG-CAT-Aurora A;p53−/−* mice were infected with adenoviral luciferase or AxCANCre and stained 72 h later with anti-α-tubulin antibodies (green) and propidium iodide (PI) to label the DNA (red). Binucleated cells and multinucleated cells (those with ⩾3 nuclei) induced by Aurora A overexpression are indicated by arrows and arrowheads, respectively. Scale bar, 20 μm. (**c**) Quantification of nuclei in primary MEFs prepared from *CAG-CAT-Aurora A;p53+/+* and *CAG-CAT-Aurora A;p53−/−* mice at 72 h after virus infection (Luc or Cre). Values shown are the mean percentages of binucleated or multinucleated cells (with ⩾3 nuclei) from three independent experiments in which > 300 cells were counted. $^*P<0.01$. (**d**) Flow cytometry of MEFs with overexpressed Aurora A. Primary MEFs from *CAG-CAT-Aurora A;p53+/+* and *CAG-CAT-Aurora A;p53−/−* mice were treated with bromodeoxyuridine (BrdU) for 4 h at 48 h after infection with AxCANCre. The percentages of BrdU-positive polyploid (DNA > 4N) cells after Aurora A overexpression were 3.55% in *CAG-CAT-Aurora A;p53+/+* MEFs and 13.58% in *CAG-CAT-Aurora A;p53−/−* MEFs.

Aurora A overexpression leads to precancerous lesions in p53-deficient mice

To investigate whether Aurora A overexpression leads to the formation of mammary tumors, female *CAG-CAT-Aurora A;Wap-Cre;p53+/−* and *CAG-CAT-Aurora A;Wap-Cre;p53−/−* mice were mated with male C57BL/6 mice and monitored weekly for the development of mammary tumors. In total 5 of 21 *CAG-CAT-Aurora A;Wap-Cre;p53+/−* mice and 5 of 11 *CAG-CAT-Aurora A;Wap-Cre;p53−/−* mice developed precancerous lesions that were histologically similar to atypical ductal hyperplasia (ADH) in human mammary tissue (Figure 2b). Hematoxylin and eosin (H&E) staining of the lesions showed increased numbers of abnormal cells within ducts or lobules and disruption of the dual-layer architecture of the mammary gland. However, these lesions lacked characteristics of invasive carcinoma such as cellular and nuclear pleomorphisms

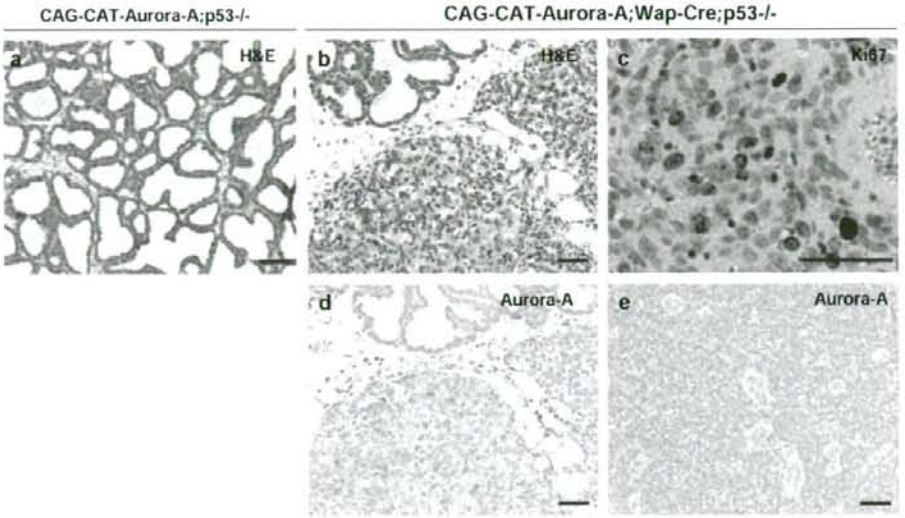

Figure 2 Wap-Cre-mediated Aurora A overexpression leads to lesions resembling atypical ductal hyperplasia (ADH) in mammary glands of p53-deficient mice. (**a**) Hematoxylin and eosin staining (H&E) of a paraffin-embedded mammary gland section from a *CAG-CAT-Aurora A;p53−/−* mouse. (**b**) H&E staining of a mammary gland section from a *CAG-CAT-Aurora A;Wap-Cre;p53−/−* mouse showing ADH-like hyperplastic lesion. (**c**) Immunohistochemical analysis of Ki67 expression in ADH-like hyperplastic lesion from tissue in (**b**). (**d**) Immunohistochemical analysis of an ADH-like lesion in mammary gland of a *CAG-CAT-Aurora A;Wap-Cre;p53−/−* mouse shows high expression of exogenous human Aurora A. (**e**) Immunohistochemical analysis of a lymphoma in the mammary gland of a *CAG-CAT-Aurora A;Wap-Cre;p53−/−* mouse shows that lymphoma cells do not express human Aurora A. Scale bars, 50 μm.

and disruption of basement membrane. In contrast, no ADH-like lesions were found in 20 *CAG-CAT-Aurora A;p53+/−* mice or in 11 *CAG-CAT-Aurora A;p53−/−* mice, which do not express Aurora A (Figure 2a). Although our previous study showed that *CAG-CAT-Aurora A;Wap-Cre;p53+/+* mice developed small papillary hyperplasia, none of them had ADH-like tumors in their mammary glands (Table 1). Additionally, immunohistochemical analysis revealed that approximately 8% of cells in these ADH-like lesions expressed the proliferation marker Ki67 (Figure 2c). However, in *CAG-CAT-Aurora A;Wap-Cre;p53+/+* mice, Ki67-positive cells were rarely detected (<1%) (Supplementary Figure S4). These data indicate that Aurora A overexpression induces cell proliferation in *p53−/−* mammary glands more than in *p53+/+* mammary glands, while not as aggressive as malignant tumors. Exogenous Aurora A levels were high in the ADH-like tumor lesions and adjacent normal mammary epithelium (Figure 2d), but lymphoma and sarcoma lesions (which often develop in *p53−/−* mice) did not express exogenous Aurora A (Figure 2e). Taken together, these results suggest that Aurora A overexpression can induce benign tumors in mammary glands when p53 function are impaired, but it is not sufficient for the development of invasive malignant tumors.

Table 1 Incidence of ADH-like tumor formation in the mammary glands of Aurora A conditional transgenic mice with different p53 background

Mouse genotype	*Tumor incidence, No. of mice (%)*	*Age of mice (days ± s.d.)*
CAG-CAT-Aurora A;Wap-Cre;p53+/+	0 of 14 (0)	512 ± 63.2
CAG-CAT-Aurora A;Wap-Cre;p53+/−	5 of 21 (24)	354 ± 71.2
CAG-CAT-Aurora A;Wap-Cre;p53−/−	5 of 11 (45)	137 ± 28.9[a]
CAG-CAT-Aurora A;p53+/−	0 of 20 (0)	357 ± 96.8
CAG-CAT-Aurora A;p53−/−	0 of 11 (0)	147 ± 38.0[a]

[a]Most *p53−/−* mice died of lymphoma or sarcoma within 200 days.

Cellular senescence in Aurora A-overexpressing mammary glands

Apoptosis and senescence are two cellular responses that prevent the transformation of normal cells into malignant cells under oncogenic stimulation. Given our previous observation that overexpression of Aurora A *in vivo* did not lead to malignancy in p53-deficient mice in which apoptosis was significantly inhibited, we speculated that cellular senescence was important in the prevention of malignant transformation in our mouse model. Thus, we investigated the status of apoptosis and senescence in Aurora A-overexpressing mammary glands. TdT-mediated dUTP-biotin nick-end labeling (TUNEL) and the active caspase-3 staining revealed that there are many apoptotic cells in *CAG-CAT-Aurora A;Wap-Cre;p53+/+* mice, while *CAG-CAT-Aurora A;Wap-Cre;p53−/−* mice had few apoptotic cells (Figure 3a; Supplementary Figure S5), which was consistent with our previous study (Zhang *et al*., 2004). Endogenous senescence-associated β-galactosidase (SA-β-gal) activity, a well established

marker of cellular senescence (Dimri *et al*., 1995), was found in response to Wap-Cre-mediated Aurora A overexpression in the mammary glands of both *p53+/+* and *p53−/−* mice, but both the amount of SA-β-gal activity and the numbers of SA-β-gal-positive cells in the *p53−/−* mice were much higher than those in *p53+/+* mice (Figures 3a and b). Senescent cells are also known to exhibit distinct senescence-associated heterochromatic foci containing heterochromatin proteins such as HP1 (Narita *et al*., 2003); they also upregulated expression of proteins such as Decoy receptor 2 (DcR2), a new oncogene-induced senescence

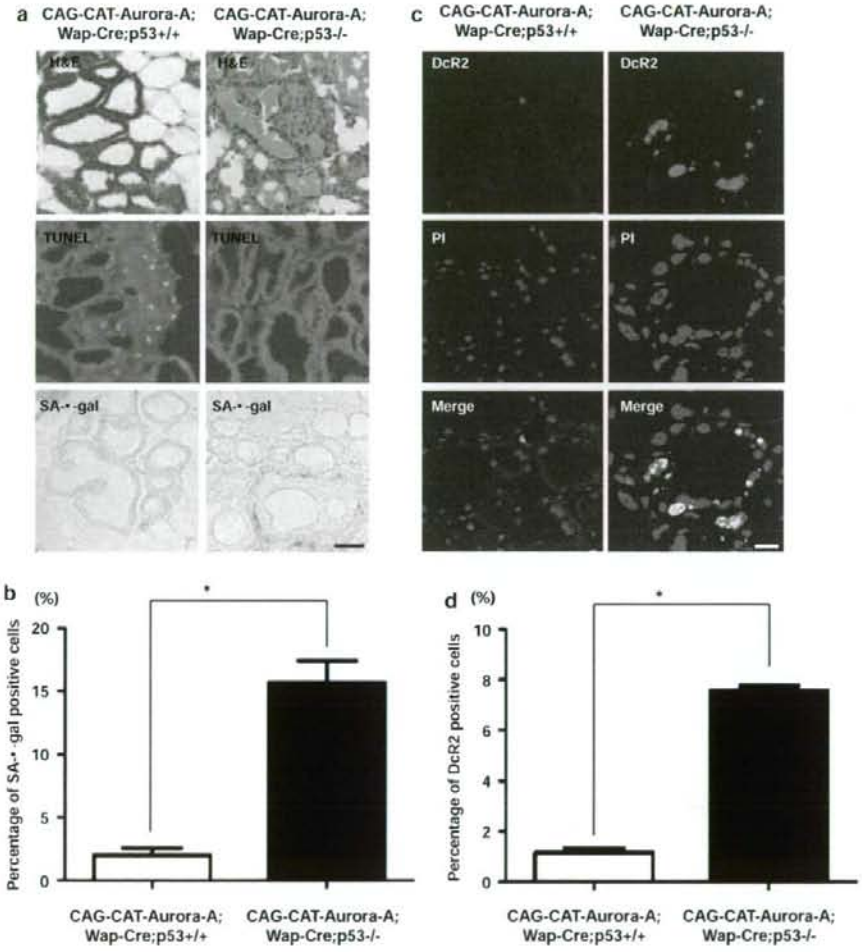

Figure 3 Mammary epithelial cells overexpressing Aurora A are positive for markers of cellular senescence. (**a**) Hematoxylin and eosin staining (H&E), TdT-mediated dUTP-biotin nick-end labeling (TUNEL) and senescence-associated β-galactosidase (SA-β-gal) assay were performed on frozen sections from mammary glands of *CAG-CAT-Aurora A;Wap-Cre;p53+/+* (left panels) and *CAG-CAT-Aurora A;Wap-Cre;p53−/−* (right panels) mice. Cells from the *p53−/−* mice showed less apoptosis and more SA-β-gal activity than the *p53+/+* mice. Scale bar, 100 μm. (**b**) Quantification of SA-β-gal-positive cells in mammary glands of *CAG-CAT-Aurora A;Wap-Cre;p53+/+* and *CAG-CAT-Aurora A;Wap-Cre;p53−/−* mice. Values shown are the mean percentages of SA-β-gal-positive cells from three animals per experimental group in which over 300 cells were counted. The percentage of SA-β-gal-positive cells in *p53−/−* mice is much higher than those in *p53+/+* mice (15.7 ± 3.06 vs 2.0 ± 1.00%) (**P*<0.05). (**c**) Immunofluorescent staining of Decoy receptor 2 (DcR2) expression. Mammary glands from a *CAG-CAT-Aurora A;Wap-Cre;p53+/+* mouse (left panels) and a *CAG-CAT-Aurora A;Wap-Cre;p53−/−* mouse (right panels) were stained with anti-DcR2 antibody (green) and DNA was visualized with propidium iodide (PI) (red). Scale bar, 20 μm. (**d**) Quantification of DcR2-positive cells in *CAG-CAT-Aurora A;Wap-Cre;p53+/+* and *CAG-CAT-Aurora A;Wap-Cre;p53−/−* mice. Values shown are the mean percentages of DcR2-positive cells from three animals per experimental group in which over 300 cells were counted. The percentage of DcR2-positive cells in *p53−/−* mice is significantly higher than those in *p53+/+* mice (7.58 ± 0.42 vs 1.15 ± 0.44%) (**P*<0.05).